# Logarithmic temperature dependence of Hall transport in granular metals

Yu-Jie Zhang,[1] Zhi-Qing Li,[1,*] and Juhn-Jong Lin[2,†]

[1]*Tianjin Key Laboratory of Low Dimensional Materials Physics and Preparing Technology, Faculty of Science,*
*Tianjin University, Tianjin 300072, China*
[2]*Institute of Physics and Department of Electrophysics, National Chiao Tung University, Hsinchu 30010, Taiwan*

We have measured the Hall coefficient $R_H$ and the electrical conductivity $\sigma$ of a series of ultrathin indium-tin-oxide films between 2 and 300 K. A robust $R_H \propto \ln T$ law is observed in a considerably wide temperature range of 2 and $\sim$120 K. This $\ln T$ dependence is explained as originating from the electron-electron interaction effect in the presence of granularity as theoretically predicted. Furthermore, we observed a $\sigma \propto \ln T$ law from 3 K up to several tens K, which also arose from the Coulomb interaction effect in inhomogeneous systems. These results provide strong experimental support for the current theoretical concepts for charge transport in granular metals with intergrain tunneling conductivity $g_T \gg 1$.

    

Granular metals are composite materials in which the metallic granules are randomly embedded in an insulating matrix. Recently, the electronic conduction properties of granular metals have attracted much renewed theoretical[1–4] and experimental[5–9] attention due to the improved nanoscale feature and rich fundamental phenomena in the presence of structural inhomogeneities. In particular, the *intragrain* electron dynamics is found to play a crucial role in the Hall transport,[4] which has often been overlooked in the everlasting studies of granular systems. Previously, great effort has long been focused on the *intergrain* electron behavior, which governs the longitudinal electrical conductivity $\sigma$.[2,3,10] In practice, an experimental detection of a many-body correction to $\sigma$ is straightforward, while a measurement of a small correction to the Hall coefficient $R_H$ in a metallic system would be a challenging task.

A granular metal refers to a granular conductor with the dimensionless intergrain tunneling conductivity $g_T = G_T/(2e^2/h) \gg 1$, where $G_T$ is the intergrain tunneling conductance, $e$ is the electronic charge, and $h$ is the Planck constant. Recently, Efetov, Beloborodov, and co-workers have carried out a series of theoretical investigations in this regime. They found that the Coulomb electron-electron ($e$-$e$) interaction effect governs the carrier transport characteristics in the presence of granularity. Kharitonov and Efetov predicted that, in the wide temperature interval of $g_T \delta \lesssim k_B T \lesssim E_0$, $R_H$ should obey[4]

$$R_H = \frac{1}{n^* e} \left[ 1 + \frac{c_d}{4\pi g_T} \ln \left( \frac{E_0}{k_B T} \right) \right], \qquad (1)$$

where $n^*$ is the effective carrier concentration, $c_d$ is a numerical lattice factor, $\delta$ is the mean-energy level spacing in the grain, $E_c$ is the charging energy, $E_0 = \min(g_T E_c, E_{Th})$, and $E_{Th}$ is the Thouless energy.

In addition, Efetov and Tschersich[2] and Beloborodov *et al.*[3] predicted that the intergrain $e$-$e$ interaction effect would cause a longitudinal electrical conductivity,

$$\sigma = \sigma_0 \left[ 1 - \frac{1}{2\pi g_T d} \ln \left( \frac{g_T E_c}{k_B T} \right) \right], \qquad (2)$$

in the temperature interval $g_T \delta < k_B T < E_c$, where $\sigma_0 = G_T a^{2-d}$ is the tunneling conductivity between neighboring grains in the absence of Coulomb interaction, $a$ is the radius of the grain, and $d$ is the dimensionality of the granular array. We note that the theories[2–4] have treated the simplest case of a regular array consisting of equally sized spherical grains (while distributions in grain size, shape, and intergrain distance always exist in real systems).

Thus far, the theoretical prediction of Eq. (1) has not been experimentally tested. The main reason is that the $n^*$ value is usually very high ($\sim 10^{28}$–$10^{29}$ m$^{-3}$) in those granular conductors made of normal-metal grains, which leads to minute $R_H$ magnitudes. Furthermore, the logarithmic correction term in Eq. (1) is predicted to be $\lesssim$10% of the total $R_H$ magnitude. Thus, an experimental test of this theoretical $R_H \propto \ln T$ law is nontrivial.

Recently, it was established that the indium-tin-oxide (ITO) material possesses free-carrier-like electronic properties.[11–14] Their resistivities could be made as low as $\rho(300 \text{ K}) \sim$ 100–200 $\mu\Omega$ cm.[14–16] Therefore, one may consider growing ultrathin ($\sim$10 nm) ITO films to form granular arrays while achieving the prerequisite condition $g_T \gg 1$. Furthermore, since the $n^*$ magnitudes in metallic ITO materials are $\sim$2 to 3 orders of magnitude lower than those in typical metals,[14] one could expect relatively large values of $R_H$. That is, the theoretical predication of Eq. (1), together with that of Eq. (2), may be tested by using granular ITO films. In this Brief Report, we show the experimental observation of the $R_H \propto \ln T$ law, as well as the $\sigma \propto \ln T$ law, in a series of ultrathin ITO films, which lie deep in the metallic regime.

Our ultrathin ITO films were deposited on glass substrates by the standard rf sputtering method. A commercial Sn-doped In$_2$O$_3$ target (99.99% purity, the atomic ratio of Sn to In being 1:9) was used as the sputtering source. The base pressure of the vacuum chamber was $\lesssim 8 \times 10^{-5}$ Pa, and the sputtering deposition was carried out in an argon atmosphere (99.999%) of 0.6 Pa. During the depositing process, the mean-film thickness $t$, together with the substrate temperature $T_s$, was varied to tune the grain size $a$ and the intergrain conductivity $g_T$ in each film. Hall-bar-shaped samples (1.5-mm wide and 1-cm long) were defined by using mechanical masks [see
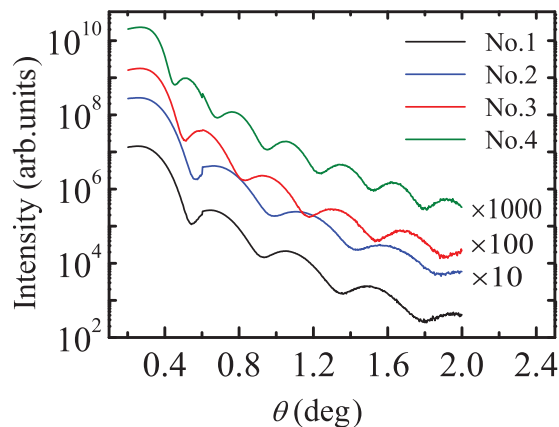
         

FIG. 1. (Color online) Low-angle x-ray diffraction patterns for four ultrathin ITO films as indicated. The data for the films Numbers 2–4 are offset for clarity.
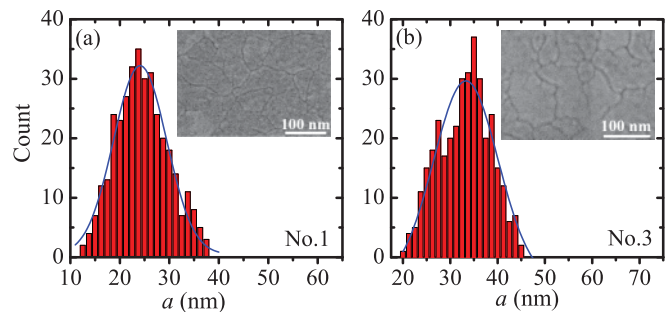


FIG. 2. (Color online) Grain-size distribution histograms for the ITO films (a) Number 1 and (b) Number 3. The insets show the corresponding SEM images.

the schematic in the inset of Fig. 3(a)]. The thicknesses of the films were measured by the low-angle x-ray diffraction (X'pertPRO multipurpose diffractometer). The surface morphologies of the films were characterized by the scanning electron microscopy [(SEM), Hitachi S-4800]. The four-probe electrical conductivity and Hall effect measurements were carried out on a physical property measurement system (PPMS-6000, Quantum Design). For $R_H$ measurements, in order to cancel out any undesirable misalignment voltages, and thermomagnetic effect, a square-wave current operating at a frequency of 8.33 Hz was applied, and the magnetic field was regulated to sweep from $-2$ to 2 T in a step of 0.05 T.

Figure 1 shows the low-angle x-ray diffraction patterns of four representative films as indicated. The relation between the position of the low-angle diffraction peak $\theta_m$ and film thickness $t$ is given by the modified Bragg equation:[17] $\sin^2(\theta_m) = (q\lambda/2t)^2 + 2\xi$, where $\lambda$ is the x-ray wavelength (the Cu K$_\alpha$ radiation), $q$ is the integer reflection order number, and $\xi$ is the average deviation of the refractive index from unity. The $t$ value of each film has been determined from the linear regression of $\sin^2(\theta_m)$ versus $q^2$ and is listed in Table I.

Figures 2(a) and 2(b) show the grain-size distribution histograms for two representative films, as indicated. The insets show the corresponding SEM images, which indicate the irregular shape of individual grains. For each selected grain,

we measured its size at six different locations and took the average value as the diameter of the grain, i.e., we modeled the grain as a disk-shaped grain with a height $t$. The distribution data were fitted with the standard Gaussian function (solid curves) to determine the mean-grain radius $a$ in each film (see Table I).

Figures 3(a)–3(d) plot the variation in Hall coefficient $R_H$ with the logarithm of temperature for four representative films, as indicated. All samples reveal negative $R_H$ at all $T$, indicating electron conduction in the ITO material.[11,14] It is clearly seen that the Hall coefficient obeys the $R_H \propto \ln T$ law between 2 K and $T_{\max}$, where $T_{\max}$ is the temperature below which the logarithmic law holds. Our experimental $T_{\max}$ values vary from $\sim 50$ to $\sim 120$ K for films Numbers 1–5 (see Table I).

Our measured $R_H$ variations with $\ln T$ were least-squares fitted to the predictions of Eq. (1), and the fitted results (straight solid lines) were plotted in Figs. 3(a)–3(d). Note that the $n^*$ value in Eq. (1) is given by the measured value between 180 and 250 K for each film, and thus, is not adjustable. (In this high-$T$ regime, the Coulomb interaction effect causes a negligible correction to $R_H$.[4]) Our extracted $n^*$ values listed in Table I are in good accord with those previously measured in homogeneous ITO films.[14] Among the three adjusting parameters $E_0$, $c_d$, and $g_T$, the $g_T$ value can be determined independently by comparing the measured $\sigma(T)$ with the prediction of Eq. (2) (see below). Our fitted values of $E_0$ and $c_d$, together with the values of $g_T$ and $T_{\max}$, are listed in Table I. Figures 3(a)–3(d) demonstrate that the predictions of Eq. (1) can well describe the experimental data over approximately

TABLE I. Sample parameters for six ultrathin ITO films. $T_s$ is the substrate temperature during deposition, $t$ is the mean-film thickness, $a$ is the mean-grain radius determined from Fig. 2, and $n^*$ is the measured effective carrier concentration. $c_d$ and $E_0$ ($\sigma_0$ and $g_T$) are adjusting parameters in Eq. (1) [Eq. (2)]. $\delta$ is the calculated mean-energy level spacing. The theoretical Thouless energy is $E_{\mathrm{Th}}^{\mathrm{th}} = \hbar D/a^2$, the experimental charging energy is $E_c = 10 k_B T^*$, and the theoretical charging energy is $E_c^{\mathrm{th}} = e^2/(8\pi\epsilon_0 a)$. The standard deviations of $a$ for films Numbers 1–4 (5 and 6) are $\approx 20\%$ ($\approx 25\%$). The uncertainties are $\approx 15\%$ in $E_0$ and $T^*$, a factor of $\sim 2$ in $\delta$, $E_{\mathrm{Th}}^{\mathrm{th}}$, and $E_c^{\mathrm{th}}$, and $\lesssim 5\%$ in other parameters.

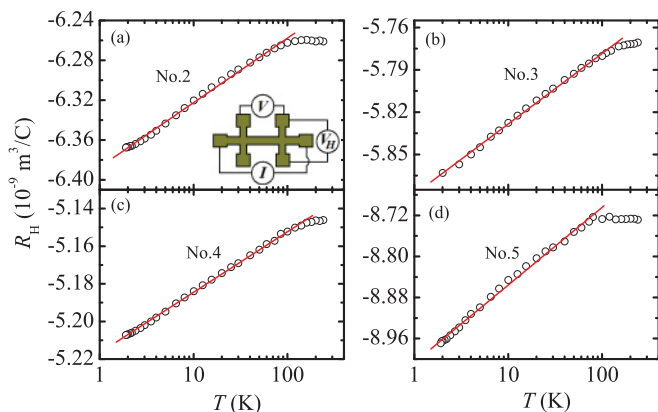| Film | $T_s$ (K) | $t$ (nm) | $a$ (nm) | $\rho(300\,\mathrm{K})$ ($\mu\Omega$ cm) | $n^*$ ($10^{27}$ m$^{-3}$) | $T_{\max}$ (K) | $c_d$ | $E_0$ ($10^{-21}$ J) | $\delta$ ($10^{-24}$ J) | $E_{\mathrm{Th}}^{\mathrm{th}}$ ($10^{-22}$ J) | $T^*$ (K) | $\sigma_0$ ($10^5$ S/m) | $g_T$ | $E_c$ ($10^{-21}$ J) | $E_c^{\mathrm{th}}$ ($10^{-21}$ J) |
|------|------|------|------|------|------|------|------|------|------|------|------|------|------|------|------|
| 1 | 610 | 9.7 | 24 | 333 | 1.1 | 85 | 0.72 | 1.3 | 3.8 | 1.5 | 46 | 3.2 | 13 | 6.3 | 4.8 |
| 2 | 630 | 9.2 | 28 | 302 | 1.0 | 73 | 0.72 | 1.3 | 2.6 | 1.3 | 48 | 3.6 | 13 | 6.6 | 4.1 |
| 3 | 650 | 11.3 | 34 | 259 | 1.1 | 100 | 1.1 | 2.0 | 1.7 | 1.0 | 49 | 4.2 | 23 | 6.8 | 3.4 |
| 4 | 670 | 13.4 | 38 | 226 | 1.2 | 120 | 1.0 | 2.1 | 1.2 | 0.90 | 50 | 4.8 | 31 | 6.9 | 3.0 |
| 5 | 650 | 7.6 | 24 | 501 | 0.73 | 50 | 0.70 | 0.99 | 5.1 | 1.2 | 55 | 2.4 | 7.4 | 7.6 | 4.8 |
| 6 | 650 | 5.4 | 22 | 839 | 0.58 | 25 | 1.0 | 0.66 | 9.4 | 1.4 | 62 | 1.5 | 4.5 | 8.6 | 5.2 |

FIG. 3. (Color online) Hall coefficient as a function of logarithm of temperature for four ITO films, as indicated. The solid straight lines are least-squares fits to Eq. (1). The inset in (a) depicts a schematic for our Hall-bar-shaped sample.

two decades of temperature in all films, strongly suggesting that the *e*-*e* interaction effect does play an important role in the Hall transport of granular metals. Our experimental results illustrate that the film thickness $t$, rather than the substrate temperature $T_s$, plays a more dominant role in governing the variation in samples' parameters.

According to Kharitonov and Efetov,[4] Eq. (1) is valid in the temperature range $g_T \delta \lesssim k_B T \lesssim E_0$. ($E_0 = E_{Th}$ in this paper.) The mean-energy level spacing $\delta$ in a single grain is given by $\delta = (\nu V)^{-1}$, where $V$ is the volume of the grain and $\nu$ is the electronic density of states at the Fermi energy. Since ITO possesses a free-electron-like band structure,[11,14] we write $\nu = m^* k_F / (\pi \hbar)^2$, where the Fermi wave number is $k_F = (3\pi^2 n^*)^{1/3}$ and the effective electron mass is $m^* = 0.55 m_e$ ($m_e$ is the free-electron mass).[18] Our calculated values of $\delta$ are listed in Table I. From Table I, one readily obtains that the lower limit in $T$, for Eq. (1) to be applicable, is $g_T \delta / k_B \sim 2$ to 3 K in all samples. This is in good consistency with our experimental observation. Furthermore, our extracted $T_{max}$ values satisfy the condition $k_B T_{max} \lesssim E_0$. However, our experimental $E_0$ values are approximately ten times

greater than the theoretical values of the Thouless energy $E_{Th}^{th} = \hbar D / a^2$,[19] where $D = \sigma / (\nu e^2)$ is the electron-diffusion constant. This underestimate of $E_{Th}^{th}$ (partly) can be explained. To accurately evaluate $E_{Th}^{th}$ from $D$, one should have used the intrinsic conductivity $\sigma_{grain}$ of an individual ITO grain, instead of using the measured $\sigma$ of the film. Therefore, the $E_{Th}^{th}$ values listed in Table I only represent the lower bounds because $\sigma_{grain} > \sigma$ in a granular array. The fact that our grains are disk shaped, but not spherical, could have introduced additional uncertainties in the estimate. In short, our measured $\ln T$ behavior of $R_H$ can be described satisfactorily by Eq. (1).

As mentioned, if the Coulomb interaction effect dominates the electron dynamics in granular ITO films, our measured $\sigma(T)$ should follow the predications of Eq. (2) in the temperature interval $g_T \delta < k_B T < E_c$. According to Efetov and Tschersich[2] and Beloborodov *et al.*,[3,20] the weak-localization (WL) effect, originally formulated for *homogeneous* systems,[21,22] should be suppressed at $T > g_T \delta / k_B$. Empirically, it has been found that the WL effect in thick ITO films could persist up to several tens K.[18] In order to fully exclude any residual WL effect on $\sigma$, we have measured $\sigma(T)$ of our ultrathin ITO films in a perpendicular magnetic field $B$ of 7 T.[20] Our results for four representative films are plotted in Fig. 4. Our measured $\sigma$ data are compared with Eq. (2), and the least-squares fitted results are plotted as the solid straight lines. Note that the prediction of Eq. (2) is valid in any $B$ as long as $\omega_c \tau < 1$, where $\omega_c$ is the cyclotron frequency and $\tau$ is the electron mean-free time.[3] In our fitting processes, $\sigma_0$ and $g_T$ are treated as adjusting parameters, and the charging energy is taken to be $E_c \approx 10 k_B T^*$,[8] where $T^*$ is the temperature below which the $\sigma \propto \ln T$ law holds (see Table I).[23] The array dimensionality is $d = 2$ in this Brief Report since our ultrathin films are nominally covered with only one layer of ITO grains. Our fitted values of $\sigma_0$ and $g_T$ are listed in Table I. Figure 4 indicates that our experimental data between $\sim 3$ K and $T^*$ are well described by Eq. (2). The values of $E_c \approx 10 k_B T^*$ are comparable to the theoretical estimates $E_c^{th} = e^2 / (8\pi \epsilon_0 a)$ within experimental uncertainties, where $\epsilon_0$ is the permittivity of vacuum. For films Numbers 1–4, our extracted $g_T$ values are far greater than 1, while for film Number 6, $g_T \simeq 4.5$. This latter value suggests that even the thinnest film Number 6 lies in the metallic region. Thus, Eqs. (1) and (2) are safely applicable for our films.
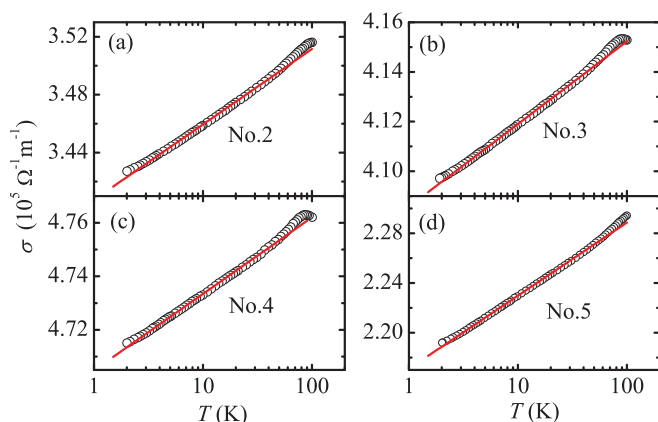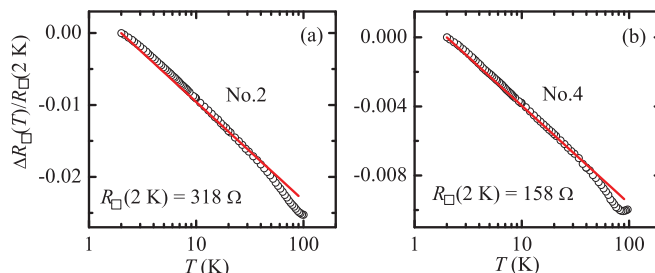


FIG. 4. (Color online) Variation in longitudinal electrical conductivity with a logarithm of temperature for four ITO films measured in a perpendicular magnetic field of 7 T. The solid straight lines are least-squares fits to Eq. (2).



FIG. 5. (Color online) Normalized sheet resistance $\Delta R_\square(T)/R_\square(2\,K)$ as a function of a logarithm of temperature in a perpendicular magnetic field of 7 T for two ITO films as indicated. The solid straight lines are least-squares fits to the two-dimensional homogeneous *e*-*e* interaction theory.

It is well known that the *e-e* interaction effect also results in a small $\ln T$ correction to longitudinal conductivity (or resistivity) in two-dimensional systems at low $T$.[22] The correction to the sheet resistance $R_\square$, due to the *e-e* interaction effect in a homogeneous weakly disordered film, is given by[22,24] $\Delta R_\square(T)/R_\square(T_0) = -(e^2/2\pi^2\hbar)(1-3\tilde{F}/4) R_\square(T_0)\ln(T/T_0)$, where $\tilde{F}$ is a screening factor and $T_0$ is an arbitrary reference temperature. Figure 5 shows the normalized sheet resistance $\Delta R_\square(T)/R_\square(2\text{ K}) = [R_\square(T) - R_\square(2\text{ K})]/R_\square(2\text{ K})$ for films Numbers 2 and 4 measured in a perpendicular $B$ of 7 T as a function of $\ln T$. (The rest of the films behave in a similar manner.) The solid straight lines are the least-squares fits to this theory. Although an approximate $\ln T$ regime seems to exist for $T$ below $\sim 35$ K, our fitted values of $\tilde{F}$ are $-0.61$ and $-0.35$ for films Numbers 2 and 4, respectively. Since this *e-e* interaction theory requires that $0 \lesssim \tilde{F} \lesssim 1$,[22] the seemingly good fits shown in Fig. 5, thus, are spurious. That is, our measured $\sigma \propto \ln T$ law in ultrathin ITO films cannot be ascribed to the conventional *e-e* interaction effect in homogeneous systems.

In conclusion, we have studied the temperature dependences of the Hall coefficient and longitudinal conductivity in a series of ultrathin ITO films. The films were specifically made granular, while possessing overall metallic behavior. We observed the robust $R_H \propto \ln T$ law, together with the $\sigma \propto \ln T$ law, over nearly two decades of temperature below $\sim 100$ K. Our results are fairly quantitatively understood within these recent theoretical frameworks of the electron-electron interaction effect in the presence of granularity. It is meditative that these theories, which are formulated based on a regular array of spheres, can be applied so successfully to explain real systems where distributions in grain size, shape, and intergrain distance exist.

*zhiqingli@tju.edu.cn

†jjlin@mail.nctu.edu.tw

[1] I. S. Beloborodov *et al.*, Rev. Mod. Phys. **79**, 469 (2007).

[2] K. B. Efetov and A. Tschersich, Phys. Rev. B **67**, 174205 (2003); Europhys. Lett. **59**, 114 (2002).

[3] I. S. Beloborodov, K. B. Efetov, A. V. Lopatin, and V. M. Vinokur, Phys. Rev. Lett. **91**, 246801 (2003).

[4] M. Y. Kharitonov and K. B. Efetov, Phys. Rev. Lett. **99**, 056803 (2007); Phys. Rev. B **77**, 045116 (2008).

[5] X. X. Zhang, C. Wan, H. Liu, Z. Q. Li, P. Sheng, and J. J. Lin, Phys. Rev. Lett. **86**, 5562 (2001).

[6] Y. N. Wu, Z. Q. Li, and J. J. Lin, Phys. Rev. B **82**, 092202 (2010).

[7] M. Huth *et al.*, New J. Phys. **11**, 033032 (2009).

[8] Y. C. Sun, S. S. Yeh, and J. J. Lin, Phys. Rev. B **82**, 054203 (2010).

[9] A. Gondorf, M. Geller, J. Weißbon, A. Lorke, M. Inhester, A. Prodi-Schwab, and D. Adam, Phys. Rev. B **83**, 212201 (2011).

[10] B. Abeles *et al.*, Adv. Phys. **24**, 407 (1975); P. Sheng, Philos. Mag. B **65**, 357 (1992).

[11] O. N. Mryasov and A. J. Freeman, Phys. Rev. B **64**, 233111 (2001).

[12] Z. Ovadyahu and Y. Imry, Phys. Rev. B **24**, 7439 (1981).

[13] X. D. Liu *et al.*, J. Appl. Phys. **104**, 073711 (2008).

[14] Z. Q. Li and J. J. Lin, J. Appl. Phys. **96**, 5918 (2004); C. Y. Wu *et al.*, *ibid.* **108**, 123708 (2010).

[15] Y. W. Hsu, S. P. Chiu, A. S. Lien, and J. J. Lin, Phys. Rev. B **82**, 195429 (2010); S. P. Chiu *et al.*, Nanotechnology **20**, 105203 (2009).

[16] E. J. Guo *et al.*, Appl. Phys. Lett. **98**, 011905 (2011).

[17] B. K. Agarwal, *X-Ray Spectroscopy* (Springer, Berlin, 1979), p. 134.

[18] T. Ohyama *et al.*, J. Phys. Soc. Jpn. **52**, 3571 (1983).

[19] D. J. Thouless, Phys. Rep. **13**, 93 (1974).

[20] I. S. Beloborodov, A. V. Lopatin, and V. M. Vinokur, Phys. Rev. B **70**, 205120 (2004).

[21] G. Bergmann, Phys. Rep. **107**, 1 (1984); Int. J. Mod. Phys. B **24**, 2015 (2010).

[22] B. L. Altshuler and A. G. Aronov, in *Electron-Electron Interactions in Disordered Systems*, edited by A. L. Efros and M. Pollak (Elsevier, Amsterdam, 1985).

[23] Our $T^*$ values are lower than the corresponding $T_{\max}$ values in those most metallic films Numbers 1–4 because the contribution from the electron-phonon scattering to $\sigma$ (but not to $R_H$) becomes progressively notable as $T \gtrsim 50$ K.

[24] J. J. Lin and N. Giordano, Phys. Rev. B **35**, 545 (1987).